scientific reports

Check for updates

OPEN

D-Glutamate production by stressed *Escherichia coli* gives a clue for the hypothetical induction mechanism of the ALS disease

Edna Ben-Izhak Monselise[1]✉, Maria Vyazmensky[1], Tali Scherf[2], Albert Batushansky[3] & Itzhak Fishov[1]✉

In the search for the origin of Amyotrophic Lateral Sclerosis disease (ALS), we hypothesized earlier (Monselise, 2019) that D-amino acids produced by stressed microbiome may serve as inducers of the disease development. Many examples of D-amino acid accumulation under various stress conditions were demonstrated in prokaryotic and eukaryotic cells. In this work, wild-type *Escherichia coli*, members of the digestive system, were subjected to carbon and nitrogen starvation stress. Using NMR and LC–MS techniques, we found for the first time that D-glutamate accumulated in the stressed bacteria but not in control cells. These results together with the existing knowledge, allow us to suggest a new insight into the pathway of ALS development: D-glutamate, produced by the stressed microbiome, induces neurobiochemical miscommunication setting on C1q of the complement system. Proving this insight may have great importance in preventive medicine of such MND modern-age diseases as ALS, Alzheimer, and Parkinson.

Keywords D-glutamate and D-glutamate racemase, Mitochondria, Eukaryotic and prokaryotic communication, Evolutionary approach

Abbreviations

GM	Gut microbiota
ALS	Amyotrophic lateral sclerosis
C1q	Complement component 1q
LC–MS	Liquid chromatography mass spectrometry
UPLC	Ultra performance liquid chromatography
HSQC	Heteronuclear single quantum correlation
NMR	Nuclear magnetic resonance

D-amino acids are indispensable for bacterial growth as components of cell wall peptidoglycans. They are incorporated into the peptidoglycan monomeric units by the MurD enzyme[1,2]. The interconversion between D- and L-glutamate is achieved by the Glutamate Racemase enzyme[3], specific for bacteria. This enzyme appears to be the primary source of D-glutamate for cell-wall biosynthesis, making it a potentially attractive target for antimicrobial drug design[4,5].

Advanced analytical techniques that detect chiral amino acids, e.g.[6] (and see[7] for a review), have demonstrated the presence of several D-amino acids in mammals as well, including humans[8,9], with identified physiological functions comprising regulatory roles (reviewed in[10]). Particularly, D-serine regulates nervous signaling in the cerebral cortex and participates in memorization and learning; D-aspartate is often present in the central nervous system (CNS), neuroendocrine, and endocrine systems and plays physiological roles in the regulation of

[1]Department of Life Science, Bergman Campus, Ben-Gurion University of the Negev, 8441901 Beer-Sheva, Israel. [2]Department of Chemical Research Support, The Weizmann Institute of Science, 7610001 Rehovot, Israel. [3]Ilse Katz Institute for Nanoscale Science & Technology, Marcus Campus, Ben-Gurion University of the Negev, 8410501 Beer-Sheva, Israel. ✉email: bened@post.bgu.ac.il; fishov@bgu.ac.il

hormone secretion and steroidogenesis[11–14]. The exogenous D-amino acids are thought to be metabolized by dietary enzymes and bacterial flora[15–17]. In eukaryotic cells, D-glutamate is metabolized within the mitochondria and chloroplasts (ancient prokaryote)[18,19]. D-Amino acids are increasingly being recognized as important signaling molecules in the central nervous system in mammals, including humans[20,21].

Abnormal levels of D-amino acids have been associated with the pathogenesis of different diseases, including schizophrenia and amyotrophic lateral sclerosis (ALS), indicating that D-amino acid levels hold potential as diagnostic markers[22–26] Table 1 summarizes 19 examples of D-amino acids' appearance under various stress or disease conditions, indicating that this phenomenon is common for prokaryotic and eukaryotic cells.

Previously, we hypothesized that the stressed microbiome may produce elevated levels of D-amino acids[48]. Emerging evidence has demonstrated that the gut microbiome (GM) plays an essential role in the pathogenesis of human diseases in distal organs[49–54]. An increasing number of studies suggested that GM can modulate nervous, endocrine, and immune communication through the gut-brain axis which takes part in the occurrence and development of central nervous system diseases. The relationship between GM and neurodegenerative disease has recently gained a lot of attention in the medical community, especially in Parkinson's and Alzheimer's diseases, and ALS[48,55–60]. A comparison between ALS and a healthy group revealed a variation in the intestinal microbial composition with a higher abundance of *E. coli* and enterobacteria and a low abundance of total yeast in patients[61]. Notably, elevated levels of D-glutamate were found in the gut microbiota of Alzheimer's disease patients[60].

This work aimed to examine D-glutamate accumulation in stressed gut microbiome as predicted in our hypothesis[48]. However, the gut microbiome is extremely complex, and its composition and corresponding functionality are very diverse and dynamic even in healthy humans (see e.g.[62]). Various in vitro experimental microbiome models were explored, but none of them can provide unambiguous results (for a review see e.g.[63]). To this end, we searched for an answer to a simple question: is an accumulation of D-glutamate by a wil D-type bacterium possible in stress conditions? The bacterium chosen for this purpose was the well-studied *E. coli* B/r H266 under nutritional starvation. Using Nuclear Magnetic Resonance (NMR) spectroscopy and liqui D-chromatography mass-spectrometry (LC–MS) techniques, we found for the first time that D-glutamate accumulated in the stressed bacteria but not in control cells. In the Discussion section, we consider how this accumulation may lead to ALS development via the complementary immune system response in the frame of our hypothesis.

Results

Chiral recognition plays an important role in many fundamental interactions of living systems. Different spectroscopic methods such as fluorescence spectroscopy, mass spectrometry, and nuclear magnetic resonance (NMR) spectroscopy, have been applied to achieve the analysis of chiral enantiomeric compound[6,64,65]. In this study, we employed targeted analysis of amino acids by liqui D-chromatography mass-spectrometry (LC–MS) and NMR spectroscopy. Since both techniques are achiral methods, chiral enantiomeric discrimination requires the formation of diastereoisomeric entities, which can then be distinguished (see Materials and Methods section).

Accumulation of D-Glutamate in starved *E. coli* revealed by LC–MS analysis

Derivatization of the L- and D-glutamic acid with a chiral reagent (S)-NIFE[66,67] allows the separation of derivatized isomers chromatographically. The identity of the targets was confirmed by the exact mass-to-charge ratio recorded by a high-resolution mass spectrometer that also allows monitoring of isotopic composition, further supporting the identification. The results of the analysis are presented in Fig. 1. The data reveals the presence of L- and D-glutamate in the samples under stress conditions, while the control samples had L-glutamate only (Fig. 1E–G). Remarkably, 10-h-long stress showed a visibly stronger accumulation of D-glutamate compared to 24 h of stress. Considering the large difference in abundance between the two forms of glutamate in the biological samples, it was impossible to quantify them precisely using LC–MS. However, relative quantification of metabolites was performed by comparative analysis, calculating the peak's areas. The results support the visual observation of higher D-glutamate content after 10 h compared to 24 h of stress. Thus, the ratio between D- and L-glutamate after 10 h was 1:6, while it was 1:12 only after 24 h. These results were consistent among the analysis of three sets of samples from three independent preparations, containing two duplicates of unstressed *E. coli* (control), 10-h stressed cells, and 24-h stressed cells each.

D-Glutamate detection in *E. coli* cells by NMR spectroscopy

NMR spectroscopy is also an achiral technique that requires the creation of diastereoisomeric entities, whereby spectral differences between an antipodal pair can be recognized. For enantiomeric discrimination, an optically pure chiral reagent (chiral auxiliary) is required to convert the mixture of enantiomers into a diastereomeric mixture through in-situ formation of nonequivalent diastereomeric complexes with substrate enantiomers. NMR resonances of diastereomers are anisochronous and, therefore, can often be distinguished in the NMR spectrum. Over many years, a variety of chiral NMR auxiliaries have been introduced, e.g. tartaric acid, which is a bidentate ligand with two chiral centers forming a seven-membered chelate ring, as well as different shift reagents. In this study, D-tartrate was added to the chiral sample, and the complex was formed in situ. In an attempt to differentiate and increase chemical shift differences between D- and L-glutamate, several chiral auxiliary reagents were tested, under different experimental conditions. Aizawa et al.[68] had used Somarium Lantanide shift reagent in the presence of chiral Tartrate, pH 8. Unfortunately, under these conditions, our biological samples had precipitated, and no NMR signal was detected. Therefore, it was decided to use D-tartaric acid solely, testing different pH conditions. Best results were obtained using a threefold excess of D-tartaric acid and pH 7, conditions that were eventually used in this study.

Entry No	Type of stress/disease	Organism	The D-amino acid accumulated	References
Prokaryotic				
1	Density	Bacteria *Bacillus anthracis* (germination of fresh spore is inhibited in a density-dependent manner by D-alanine)	D-Alanine	27
2	Hyperthermal stress	Archaea *Pyrobaculum islandicum* *Methanosarcina barkeri Halobacterium salinarium*	D-Alanine	28
3	*Vibrio cholerae* mrcA mutant	Bacteria a mutant in *Vibrio cholerae* mrcA, and *Bacillus subtilis-generated*	D-Methionine D-Leucine D-Tryptophan D-Phenyl alanine	29
Eukaryotic				
4	Osmotic stress	Parasitic protozoan *Leishmania amazonensis*	D-Alanine	30
5	Hypersalinity acclimation	Crustaceans Aquatic invertebrates *Penaeus japonicus* *Procambarus clarkia* *Juasus lalandi* *Chionoecetes opili* Eriocheir japonicus	D-Alanine	31
6	Changes in external salinity	A brackish-water mollusc, Corbicula japonica	D-Alanine	32
7	Hypersalinity acclimation	Mollusks Aquatic invertebrates *Scapharca broughtonii* *Crassostrea gigas* *Patinopecten yessoensis* *Meretrix lusoria* *Ruditapes philippinarum* *Pseudocardium sachalinensis* *Tresus keenae*	D-Alanine	31
8	Hypertonic or Hypotonic stress	Mollusks aquatic invertebrates *Lucinoma aequizonata*	D-Alanine	33
9	Herbicides	Plant *Nicotiana tabacum*	D-Alanine	34
10	Ultraviolet radiation	Duckweed plants *Landoltia punctata*	D-Alanine	6
11	Amino acid deprivation	Plant *Arabidopsis thaliana*	D-Alanine	35
12	Tidal freshwater marshes	Plant *Phragmites australis*	D-Alanine	36
13	Most exposed to chronic mild stress (CMS), also some of them with Alzheimer's disease (AD)	Male Wistar Rats mammalian tissues frontal cortex	D-Glutamate	37
14	Mutant ddY/DAO$^-$ mice lacking D-amino-acid oxidase	Mouse mammalian tissues in the pituitary and pineal glands	D-Serine D-Alanine D-Proline D-Asparagine D-Serine D-Leucine	38–41
15	Treated with drugs employed for therapy of mood/anxiety and subjected to food shock stress	Rat mammalian tissues	D-Glutamate	42
16	Adult male-aging	Rat mammalian tissues salivary glands CNS anterior pituitary gland and in the pancreas Islets of Langerhans of rat pancreas	D-Alanine D-Asparagine D-Alanine	43–45
17	Renal–kidney disease-	Human *Homo sapiens* mammalian tissues	D-Serine D-Alanine D-Proline	46
18	Alzheimer's disease (AD)	Human	D- Serine D-Alanine D-Proline D-Glutamate	25
19	Motor Neuron Disease (MND)/Amyotrophic Lateral Sclerosis (ALS)	Human	D-Asparagine D-Glutamate	47

Table 1. D-amino acid accumulation, as signaling agents, under various stress or disease conditions-a universal phenomenon.

One-dimensional (1D) ^{1}H NMR spectra, as well as 2D ^{1}H-^{13}C Heteronuclear Single Quantum Correlation (HSQC) NMR spectra, were used to characterize and identify the presence of glutamate in stressed cell extract.

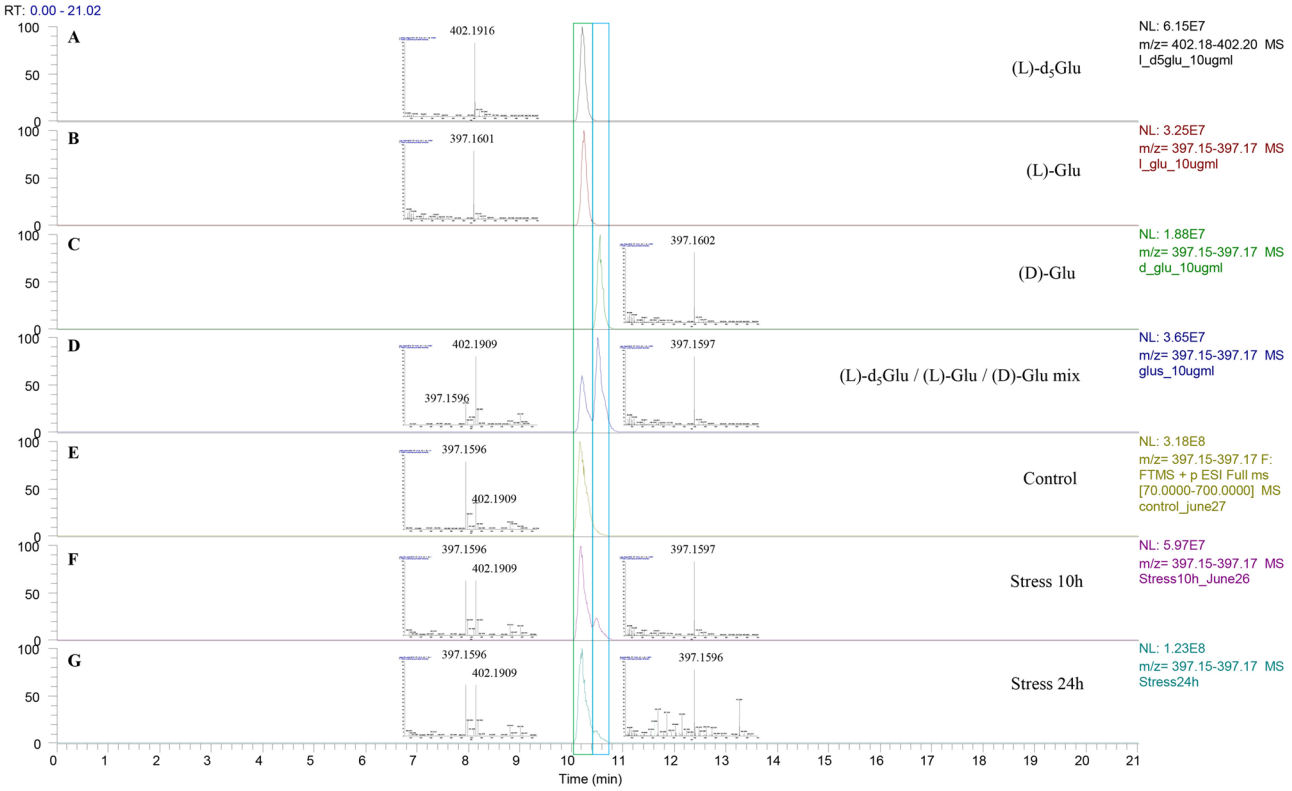

Figure 1. The results of LC–MS analysis of glutamic acids enantiomers. (**A**–**D**) Separation method development and verification; (**E**–**G**) representative samples of the control and the stress conditions. Chromatographic peaks framed in green (retention time 10.25 min) are L-glutamic acid (regular and d_5-labeled stable isotope as internal standard), and peaks framed in blue (retention time 10.55 min) are D-glutamic acid. The mass-spectrum values of the corresponding peaks are presented in the plot.

A comparison of the ^{1}H and ^{13}C chemical shifts between standard samples of D- and L-glutamate reveals slight differences between the NMR signals of the two glutamate enantiomers. The superposition of the 1D ^{1}H NMR spectra of D-glutamate (red), L-glutamate (blue), and a mixture of D- and L-glutamate, 1:15 (green), is displayed in Fig. 2. (This 1:15 ratio was chosen as the desired lowest detection level based on results obtained by LC–MS for the biological samples. Spectra of 1:1, and 1:2 mixtures are shown in the Fig. S1 of Supplementary Information.). The largest chemical shift difference is observed for the H_β signals (~2.36 ppm; see Fig. 2 insert/enlargement). Chemical shifts of the 1:15 D:L-glutamate mixture (Fig. 2) further support the chemical exchange between the two forms, revealing weighted average chemical shifts of D- and L-glutamate.

^{13}C chemical shifts differences between D- and L-glutamate followed the trend observed for the ^{1}H shift differences. To simultaneously track ^{1}H and ^{13}C shift differences, a 2D ^{1}H–^{13}C Heteronuclear Single Quantum Correlation (HSQC) NMR spectrum was recorded. Figure 3 presents the aliphatic region of the 2D ^{1}H–^{13}C correlation spectrum of stressed cell extract (red), superimposed on the corresponding spectrum of a 1:15 mixture of D- and L-glutamate (blue). For clarity, the 1D ^{1}H NMR spectrum of the latter mixture sample is shown as well (green). The chemical shifts of the 1:15 mixture signals nicely fit the signals of the stressed cell extract, clearly supporting and identifying the presence of glutamate in the cell extract sample.

Discussion

Our efforts to optimize the conditions allowing an effective resolution of NMR signals of the glutamate enantiomers led to the desired results: the presence of D-glutamate in the 24-h starved *E. coli* was unambiguously detected (Figs. 2 and 3). The similarly optimized LC–MS spectroscopy not only successfully detected D-glutamate presence in the biological samples, but also provided valuable quantitative data. We note here that some of the samples subjected to the stress conditions did not demonstrate a remarkable accumulation of D-glutamate in the range of 1:6 or 1:12 (after 10 and 24-h starvation, respectively) compared to L-glutamate as shown in Fig. 1. As well, *E. coli* as other bacterial species are known to adapt gradually to nutritional stress[69,70]. In light of this, we assume that the decrease in the D:L glutamate enantiomers ratio may reflect the adaptation process during long starvation. Nevertheless, the reliability of the results was confirmed by the consistent detection of D-glutamate in the samples in each of the three independent sets of bacterial samples. We therefore may use the highest detected D:L ratio of 1:6 to estimate the D-glutamate concentration in starved cells. The reported L-glutamate content in *E. coli* cells normally growing at the same conditions[71,72] is 64 μmol/g of dry weight. Taking the average cell volume of 3 fl, and dry weight of a single cell of 470 fg, the D-glutamate concentration within an average *E. coli*

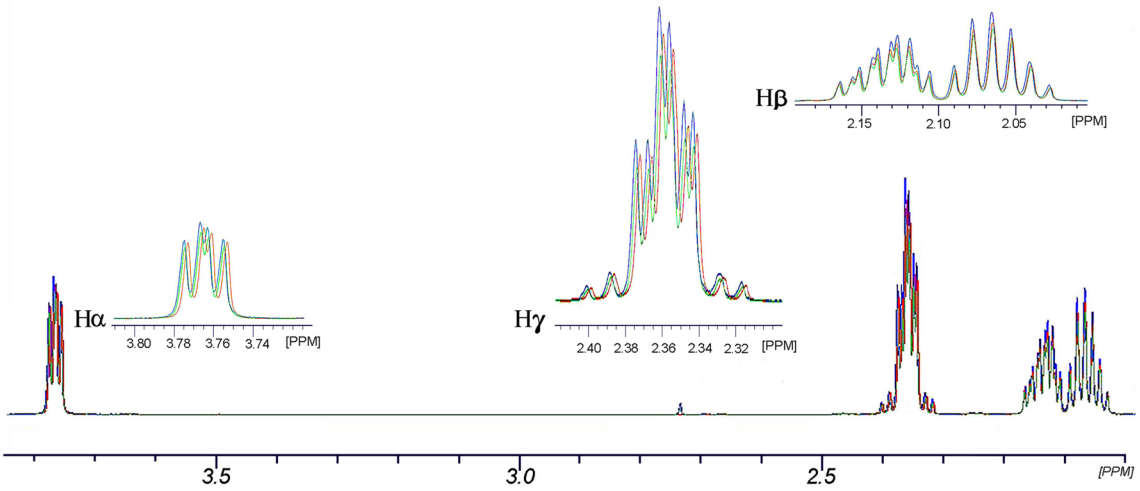

Figure 2. Superposition of 1D ^{1}H NMR spectra of D-Glu (red), L-Glu (blue) and a mixture of D- & L-Glu, 1:15 (green), all dissolved in 10/90% D_2O/H_2O, pH 7. The inserts present the enlarged signals of H_β (~2.10 ppm), H_γ (~2.36 ppm), and H_α (~3.70 ppm).

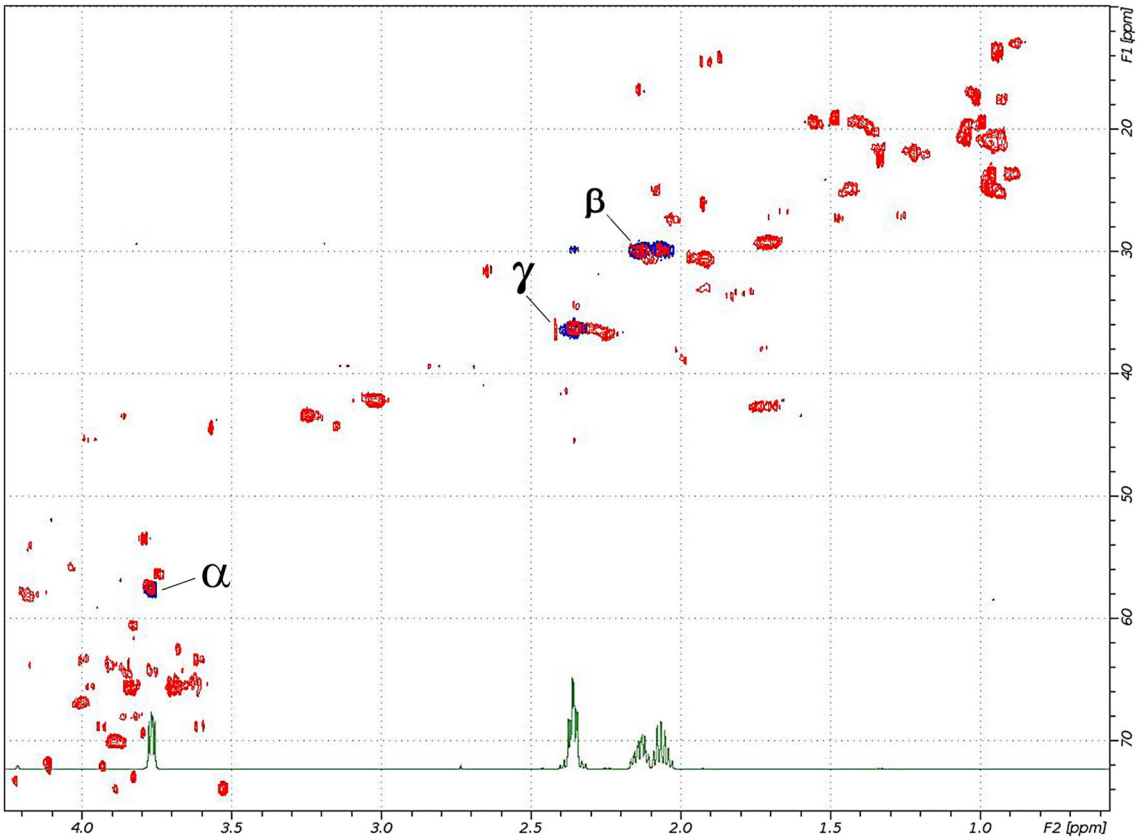

Figure 3. The aliphatic spectral region of 2D ^{1}H–^{13}C correlation NMR Spectrum of stressed cell extracts (red), superimposed on the corresponding spectrum of a mixture of D- and L-Glu, 1:15 (blue). For clarity, the 1D ^{1}H NMR spectrum of the latter is shown in the bottom (green). H/C correlation signals arising from the α, β and γ positions of glutamic acid are marked.

cell can be calculated as about 50 µM. This value looks reasonable and essential if D-glutamate is released from the starved cells that eventually lyse.

Since D-glutamate is an essential component in pathway of the peptidoglycan synthesis in bacteria, its accumulation is expected in any case of L-glutamate availability and arrested growth (e. g. about a tenfold increase in glutamate levels in *E. coli* cells with the transiently paused growth[71,73]. The constitutive glutamate racemase may readily convert L-glutamate to Denantiomer at these physiological conditions. This kind of stress-induced accumulation of D-glutamate may occur in all peptidoglycan-synthesizing bacteria populating the microbiome of the digestive system. The excretion of amino acids from bacterial cells under stress, or even at normal growth conditions[74], was demonstrated although we are not aware of the chiral specificity of the carrier.

What may be a consequence of such D-glutamate accumulation in the stressed microbiome? A hectic modern lifestyle may affect human health by causing stress to the gut microbiota. As a result, the gut microbiota releases their signaling agents, D-amino acids, as their distress beacons (see for a review[10]. Another source of D-glutamate in the digestive system arises from consumed industrial food that contains a high percentage of D-glutamate[60,75–78]. Further, D-amino acids may travel via the bloodstream throughout the entire circulatory system setting on a neurobiochemical chain reaction by exciting the Complement immune system C1q and disrupting the signaling in CNS (Fig. 4).

The complement component 1q, or briefly C1q, is a pattern recognition protein as it can identify various structures and ligands on microbial surfaces, apoptotic cells, or indirectly via antibodies and C-reactive protein[85,88–91]. The immune system can react to elevated levels of D-glutamate by initiating the classical pathway of complement activation, which can help to eliminate the bacterial D-amino acid[92] (Fig. 4). When C1q is introduced to components of a potential pathogen, it may trigger the production and activation of more C1q as part of the immune response[93]. Clinical studies[94] reveal that antibodies specific to human C1q cause a slowdown in ALS progression by reducing C1q activity/levels. Besides its role in innate immunity, C1q has a function in neurodevelopment, where it marks synapses for pruning by glia[95]. Aberrant activation of C1q in Alzheimer's disease and related conditions leads to the removal of healthy synapses and contributes to dementia and loss of function[96]. Neutralizing C1q with ANX005 aims to limit complement-mediated neurodegeneration and preserve synapses[94].

We are trying to locate and understand the source of neurobiochemical miscommunication occurring in neurodegenerative diseases such as ALS. ALS, commonly known as Lou Gehrig's disease, is characterized by progressive degeneration of both upper and lower motor neurons, resulting in muscle atrophy, gradual paralysis, and death, usually resulting from respiratory failure. Sporadic ALS has a worldwide prevalence of 6–8 in 100,000. The average age of onset is between 55 and 65 years of age. The average survival period is 2–5 years from diagnosis[97–99]. Structurally altered and aggregated mitochondria, with a swollen and vacuolated appearance, are one of the first changes observed in ALS patient motor neurons[100], suggesting direct involvement in disease pathogenesis[80]. Unfortunately, there are very few, if any, effective treatments for this disease, and of its origins. One of the mechanisms leading to nerve cell damage is the elevated Glutamate in the bloodstream. Accordingly, the main component of medicine Rilutek (riluzole) affects presynaptic sodium channels causing a reduction in the release of Glutamate[101,102].

In this study, revealing the increased levels of D-glutamate under stress conditions we have proved the first step in the hypothesis suggested earlier[103]. Further studies are required to examine the next steps in the proposed scheme of ALS disease development (Fig. 4), inspiring possible treatment or prevention. We believe it may be important in preventive medicine for many other modern-age MND diseases e.g., Alzheimer and Parkinson.

Material and methods

Strains and media

A wild strain *Escherichia coli* B/r H266[104] was grown in minimal salt M9 medium (Formedium LTD, Hunstanton, UK) supplemented with 0.2% glucose, 1 mM $MgSO_4$, 0.1 mM $CaCl_2$, and 0.1 µg/ml Thiamine (B1) (Sigma Germany), in Erlenmeyer flasks with shaking at 37 °C, for 20 h. Cells were collected by filtration using sterile Polycarbonate filters (0.4 µ pore size, 47 mm diameter) and resuspended to an OD_{600} of 1.8 in "Stress medium": growth medium without NH_4Cl and glucose, for incubation periods of either 10 h or 24 h in a shaker at 37 °C. The cells were harvested by centrifugation (1500×*G* for 15 min at 24 °C) and the pellet was stored at − 80 °C until extraction for NMR and UPLC studies.

LC–MS analysis

Targeted LC–MS analysis is a widely used technique in biological studies. It is based on separating components in a complex mixture by liquid chromatography and detecting their mass-to-charge ratio by mass-spectrometry. However, direct chromatography of enantiomers having identical molecular weight will also have the same retention time, making simple LC–MS ineffective. This challenge can be overcome using LC column with a chiral stationary phase[105]. This method requires a precise selection of specific columns, and multiple optimizations for specific compounds and still is not widely accessible for biological samples where the difference between concentrations of L- and D-amino acids can be orders of magnitude. In this study, a chemical derivatization followed by a relatively simple reverse-phase LC–MS technique demonstrated a better alternative.

Sample preparation for the LC–MS

Extraction was started by adding 2 ml of pre-chilled LC–MS grade methanol to the frozen pellet. The mixture was vortexed, thawed on ice, vortexed again, and sonicated for 5 min in the ultrasound bath. Next, 1 ml of LC–MS grade chloroform and 1 ml of LC–MS grade water were consequently added. The mixture was vigorously shaken for 10 min and centrifuged for 10 min at 14,000 rpm. The supernatant was transferred to the new Eppendorf

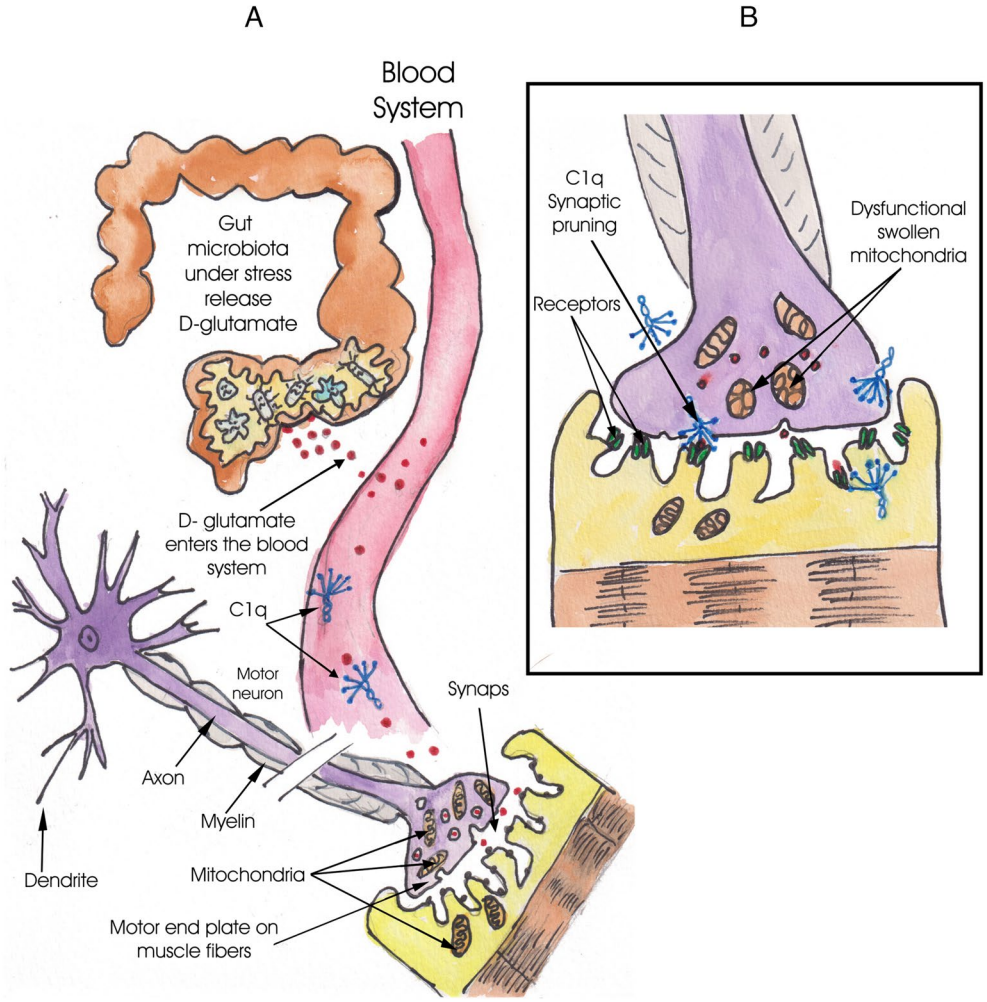

Figure 4. Scheme illustrating the connection between a stressed gut microbiota releasing D-glutamate as a communication signal, and C1q immune reaction (**A**) and the resulting impact on motor neurons (**B**). Mitochondria are of particular importance in neurons, which have high metabolic requirements. ALS-associated mitochondrial dysfunction comes in many guises, including defective oxidative phosphorylation, reactive oxygen species (ROS) production, impaired calcium buffering capacity, and defective mitochondrial dynamics[79]. Mitochondrial dysfunction is one of the earliest pathophysiological events in ALS[80] The mitochondrial ultrastructure is a useful tool for assessing mitochondrial quality[81]. Aggregated mitochondria, with a swollen and vacuolated appearance, are one of the first changes[82–84]. The activity of the complexes involved in the electron transport chain is decreased in ALS. This results in decreased ATP generation, and increased generation of ROS leading to oxidative damage to DNA, RNA and mRNA[80]. In synaptic pruning, microglia-derived C1q may play an essential source of excessive synapse removal leading to pathological conditions[85–87].

tubes and completely evaporated in the SpeedVac for 8 h[106]. The dry pellet was reconstituted in 50 µl of LC–MS grade water and subjected to derivatization.

Chiral derivatization with (S)-*N*-(4-nitrophenoxycarbonyl) phenylalanine methoxyethyl ester, (S)-NIFE, was performed based on the previously published works with modifications[66,67]. The derivatization process conjugate (S)-NIFE and amino acid (glutamate) radical, changing the targeted molecular weight (Fig. 5). Briefly, 10 µl of the sample were mixed with 10 µl of the internal standard (d_5-L-glutamate 10 µg/ml) and 20 µl of 0.15 M sodium tetraborate, briefly vortexed, and then 30 µl of 2.5 mg/ml (S)-NIFE in acetonitrile were added. The mixture was incubated for 40 min at 22 °C on the slowly rotating thermos-shaker, and then neutralized by adding 6 µl of 4 N HCl and diluted with 24 µl of water to the total volume of 100 µl. The samples were centrifuged for 5 min at 14,000 rpm, and 60 µl from the top were transferred to the LC–MS vials.

LC–MS setup

The Waters Ultra Performance Liquid Chromatography (UPLC) system coupled with Thermo Exploris 240 mass-spectrometer was used for the analysis. A separation of the derivatized compounds was achieved on Waters BEH C18 column (1.7 µm, 2.1 × 50 mm) using the following gradient of the mobile phase A (0.1% formic acid) and mobile phase B (acetonitrile): 0 min 95% A, 15 min 70% A, 15.5–17.5 min 0% A, 18–21 min 95% A. The

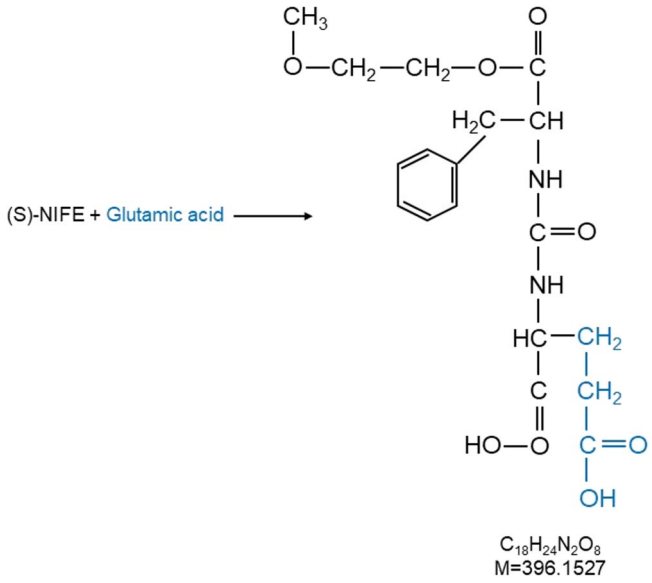

Figure 5. A scheme of chiral derivatization of glutamic acid with (S)-NIFE reagent.

injection volume was 2 µl, the column temperature was kept at 40 °C, and the flow rate was 0.2 ml/min. The total run time was 21 min.

High-resolution mass spectra were acquired using electron spray ionization (ESI) in positive full scan mode (70–700 *m/z*) with a resolution of 24,000 full width at half-maximum (FWHM). The MS parameters (ion spray voltage, sheath gas, aux gas, sweep gas, ion transfer tube temperature, and vaporizer temperature) were set up according to the manufacturer's recommendations. Data were acquired under the control of Thermo Xcalibur software version 4.5.455 (Thermo Fisher Scientific) (https://www.thermofisher.com) which was used for data analysis as well, extracting targeted ions (EIC) of the derivatized targets (L- and D-glutamate) and their internal standard (d_5-L-glutamate), and relative targets quantification.

NMR analysis

NMR sample preparation

Standard samples of D-glutamate, L-glutamate (Sigma), and their 1:1, 1:2, and 1:15 mixtures of 136 mM (in total) were prepared in the presence of threefold D-Tartaric acid, in 90%/10% H_2O/D_2O, pH 7. Chemical shift calibration standard, 3-(trimethylsilyl) propionic acid-2,2,3,3-d4 (TMSP) was added.

Biological samples were prepared from about 5×10^{10} cells collected from a liquid culture as described above. The concentrated cells were thawed and sonicated by Sonics Vibra Cell, pulse amplitude 35% for 2 min. Both control and stressed-cell samples were prepared in the presence of a threefold excess of D-Tartaric acid, in 90%/10% H_2O/D_2O, pH 7 using TMSP as a chemical shift calibration standard.

NMR spectroscopy

NMR experiments were conducted at 298 °K on a Bruker Avance NEO 600 MHz NMR spectrometer equipped with a 5-mm cryogenic triple-resonance HCN TCI probe. Data were processed and analyzed using TOPSPIN 4.0 (Bruker BioSpin, Germany). Spectra were referenced against internal sodium salt of 3-(trimethylsilyl) propionic acid-2,2,3,3-d4 (TMSP). One-dimensional ^{1}H NMR spectra were acquired using solvent presaturation to suppress the solvent signal. Two-dimensional ^{1}H–^{13}C Heteronuclear Single Quantum Coherence (2D HSQC) spectra were recorded using 8192 (t2) × 256 (t1) data points. Multiplicity editing HSQC enables differentiating between methyl and methine groups that give rise to positive correlation, versus methylene groups that appear as negative peaks.

Data availability

The datasets used and/or analysed during the current study available from the corresponding author on reasonable request.

Received: 14 March 2024; Accepted: 25 July 2024
Published online: 06 August 2024

References

1. Vollmer, W., Blanot, D. & de Pedro, M. A. Peptidoglycan structure and architecture. *FEMS Microbiol. Rev.* **32**, 149–167 (2008).
2. Barreteau, H. *et al.* Cytoplasmic steps of peptidoglycan biosynthesis. *FEMS Microbiol. Rev.* **32**, 168–207 (2008).
3. Katane, M. *et al.* Identification of an l-serine/l-threonine dehydratase with glutamate racemase activity in mammals. *Biochem. J.* **477**, 4221–4241 (2020).
4. Dodd, D. *et al.* Functional comparison of the two *Bacillus anthracis* glutamate racemases. *J. Bacteriol.* **189**, 5265–5275 (2007).

5. Spinelli, J. B. & Haigis, M. C. The multifaceted contributions of mitochondria to cellular metabolism. *Nat. Cell Biol.* **20**, 745–754 (2018).
6. Monselise, E. B., Levkovitz, A. & Kost, D. Ultraviolet radiation induces a stress effect upon etiolated *Landoltia punctata*, as evident by the universal stress signal, alanine—An ^{15}N NMR study. *Plant Biol.* **17**(1), 101–107 (2015).
7. Liu, Y., Wu, Z., Armstrong, D. W., Wolosker, H. & Zheng, Y. Detection and analysis of chiral molecules as disease biomarkers. *Nat. Rev. Chem.* **7**, 355–373 (2023).
8. Ogawa, T. K. D-amino acids in nature. *Kagaku to Seibutsu* **14**, 610–616 (1976).
9. Lau, F. S., Brennan, F. P. & Gardiner, M. D. Multidisciplinary management of motor neurone disease. *Aust. J. Gen. Pract.* **47**, 593–597 (2018).
10. Aliashkevich, A., Alvarez, L. & Cava, F. New insights into the mechanisms and biological roles of D-amino acids in complex eco-systems. *Front. Microbiol.* **9**, 683 (2018).
11. Miyoshi, Y., Oyama, T., Itoh, Y. & Hamase, K. Enantioselective sleep-awake profile related circadian D-alanine rhythm in human serum and urine. *Chromatography* (2014).
12. Miyoshi, Y., Oyama, T., Itoh, Y. & Hamase, K. Enantioselective two-dimensional high-performance liquid chromatographic determination of amino acids; analysis and physiological significance of D-amino acids in mammals. *Chromatography* **35**, 49–57 (2014).
13. Usiello, A. *et al.* New evidence on the role of D-aspartate metabolism in regulating brain and endocrine system physiology: From preclinical observations to clinical applications. *Int. J. Mol. Sci.* **21**, 8718. https://doi.org/10.3390/ijms21228718 (2020).
14. Grimaldi, M. *et al.* Prenatal and early postnatal cerebral d-aspartate depletion influences l-amino acid pathways, bioenergetic processes, and developmental brain metabolism. *J. Proteome Res.* **20**, 727–739 (2021).
15. Diven, W. F. Studies on amino acid racemases II. Purification and properties of the glutamate racemase from *Lactobacillus fermenti*. *Biochim. Biophys. Acta. B.B.A Enzymol.* **191**, 702–706 (1969).
16. Gallo, K. A. & Knowles, J. R. Purification, cloning, and cofactor independence of glutamate racemase from Lactobacillus. *Biochemistry* **32**, 3981–3990 (1992).
17. Gallo, K. A., Tanner, M. E. & Knowles, J. R. Mechanism of the reaction catalyzed by glutamate racemase. *Biochemistry* **32**, 3991–3997 (1993).
18. Ariyoshi, M. *et al.* D-Glutamate is metabolized in the heart mitochondria. *Sci. Rep.* **7**, 43911 (2017).
19. Rivera, M. C. & Lake, J. A. The ring of life provides evidence for a genome fusion origin of eukaryotes. *Nature* **431**, 152–155 (2004).
20. Wolosker, H. & Radzishevsky, I. Promiscuous enzymes generating d-amino acids in mammals: Why they may still surprise us?. *Biochem. J.* **478**, 1175–1178 (2021).
21. Souza, I. N. D. O., Roychaudhuri, R., de Belleroche, J. & Mothet, J. d-Amino acids: New clinical pathways for brain diseases. *Trends Mol. Med.* **29**, 1014–1028 (2023).
22. Visser, W. F. *et al.* A sensitive and simple ultra-high-performance-liquid chromatography-tandem mass spectrometry based method for the quantification of D-amino acids in body fluids. *J. Chromatogr. A* **1218**, 7130–7136 (2011).
23. Baumgart, F. & Rodríguez-Crespo, I. D-amino acids in the brain: The biochemistry of brain serine racemase. *FEBS J.* **275**, 3538–3545 (2008).
24. Chervyakov, A. V., Gulyaeva, N. V. & Zakharova, M. N. D-amino acids in normal ageing and pathogenesis of neurodegenerative diseases. *Neurochem. J.* **5**, 100–114 (2011).
25. Chang, C. *et al.* Plasma d-glutamate levels for detecting mild cognitive impairment and Alzheimer's disease: Machine learning approaches. *J. Psychopharmacol.* **35**, 265–272 (2021).
26. Irazoki, O. *et al.* D-amino acids signal a stress-dependent run-away response in *Vibrio cholerae*. *Nat. Microbiol.* **8**, 1549–1560 (2023).
27. McKevitt, M. T. *et al.* Effects of endogenous d-alanine synthesis and autoinhibition of *Bacillus anthracis* germination on in vitro and in vivo infections. *Infect. Immun.* **75**, 5726–5734 (2007).
28. Nagata, Y. *et al.* Occurrence of D-amino acids in a few archaea and dehydrogenase activities in hyperthermophile *Pyrobaculum islandicum*. *Biochim. Biophys. Acta.* **16**, 160–166 (1999).
29. Lam, H. *et al.* D-amino acids govern stationary phase cell wall. *Science* **325**, 1552–1555 (2009).
30. Panizzutti, R., de Souza Leite, M., Pinheiro, C. M. & Meyer-Fernandes, J. R. The occurrence of free D-alanine and an alanine racemase activity in *Leishmania amazonensis*. *FEMS Microbiol. Lett.* **256**, 16–21 (2006).
31. Abe, H., Yoshikawa, N., Sarower, M. G. & Okada, S. Physiological function and metabolism of free D-alanine in aquatic animals. *Biol. Pharm. Bull.* **28**, 1571–1577 (2005).
32. Nomura, T., Yamamoto, I., Morishita, F., Furukawa, Y. & Matsushima, O. Purification and some properties of alanine racemase from a bivalve mollusc *Corbicula japonica*. *J. Exp. Zool.* **289**, 1–9 (2001).
33. Wiley, S. & Felbeck, H. D-alanine metabolism in the lucinid Calm *Lucinoma aequizonata*. *J. Comp. Physiol. B* **164**, 561–569 (1994).
34. Gisby, M. S., Mudd, E. A. & Day, A. Growth of transplastomic cells expressing D-amino acid oxidase in chloroplasts is tolerant to D-alanine inhibited by D-valine. *Plant Physiol.* **160**, 2219–2226 (2012).
35. Gördes, D., Koch, G., Thurow, K. & Kolukisaoglu, U. Analyses of Arabidopsis ecotypes reveal metabolic diversity to convert D-amino acids. *SpringerPlus* **2**, 559 (2013).
36. Gribsholt, B., Veuger, B., Tramper, A., Middelburg, J. J. & Boschker, H. T. S. Long-term ^{15}N-nitrogen retention in tidal freshwater marsh sediment: Elucidating the microbial contribution. **54**, 13–22 (2009).
37. Martín-Hernández, D. *et al.* Chronic mild stress alters kynurenine pathways changing the glutamate neurotransmission in frontal cortex of rats. *Mol. Neurobiol.* **56**, 490–501 (2019).
38. Konno, R., Nagata, Y., Niwa, A. & Yasumura, Y. Spontaneous excretion of D-alanine in urine in mutant mice lacking D-amino-acid oxidase. *Biochem. J.* **1**, 285–287 (1989).
39. Konno, R., Niwa, A. & Yasumura, Y. Intestinal bacterial origin of D-alanine in urine of mutant mice lacking D-amino-acid oxidase. *Biochem. J.* **268**, 263–265 (1990).
40. Nagata, Y. *et al.* The presence of free D-alanine D-proline and D-serine in mice. *Biochim. Biophys. Acta BBA Gen. Subj.* **1115**, 208–211 (1992).
41. Nagata, Y., Konno, R. & Niwa, A. Amino acid levels in D-alanine-administered mutant mice lacking D-amino acid oxidase. *Metabolism* **43**, 1153–1157 (1994).
42. Musazzi, L. *et al.* Acute stress increases depolarization-evoked glutamate release in the rat prefrontal/frontal cortex: the dampening action of antidepressants. *PLoS One* **5**, e8566 (2010).
43. Masuda, W., Nouso, C., Kitamura, C., Terashita, M. & Noguchi, T. Free D-aspartic acid in rat salivary glands. *Arch. Biochem. Biophys.* **1**, 46–54 (2003).
44. Morikawa, A., Hamase, K. & Zaitsu, K. Determination of D-alanine in the rat central nervous system and periphery using column-switching high-performance liquid chromatography. *Anal. Biochem.* **312**(1), 66–72 (2003).
45. Ota, N., Rubakhin, S. S. & Sweedler, J. V. D-Alanine in the islets of langerhans of rat pancreas. *Biochem. Biophys. Res. Commun.* **2**, 328–333 (2014).

46. Lin, C. H., Yang, H. T., Chiu, C. C. & Lane, H. Y. Blood levels of D-amino acid oxidase vs. D-amino acids in reflecting cognitive aging. *Sci. Rep.* **7**, 14849 (2017).
47. Paul, P. & de Belleroche, J. The role of D-amino acids in amyotrophic lateral sclerosis pathogenesis: a review. *Amino Acids* **43**, 1823–1831 (2012).
48. Monselise, E. B. I. D-amino acids are signaling agents under stress, that broadly impact preventive medicine. *Preprints* 2019090334 (2019).
49. Pellegrini, C., Antonioli, L., Colucci, R., Blandizzi, C. & Fornai, M. Interplay among gut microbiota, intestinal mucosal barrier and enteric neuro-immune system: A common path to neurodegenerative diseases?. *Acta Neuropathol.* **136**, 345–361 (2018).
50. Blacher, E. *et al.* Potential roles of gut microbiome and metabolites in modulating ALS in mice. *Nature* **572**, 474–480 (2019).
51. Kundu, P., Blacher, E., Elinav, E. & Pettersson, S. Our gut microbiome: The evolving inner self. *Cell* **171**, 1481–1493 (2017).
52. Suez, J. *et al.* Artificial sweeteners induce glucose intolerance by altering the gut microbiota. *Nature* **514**, 181–186 (2014).
53. Ojeda, J., Ávila, A. & Vidal, P. M. Gut microbiota interaction with the central nervous system throughout life. *J. Clin. Med.* **10**, 1299 (2021).
54. Gerhardt, S. & Mohajeri, M. H. Changes of colonic bacterial composition in Parkinson's disease and other neurodegenerative diseases. *Nutrients* **10**, 708 (2018).
55. Zhu, S. *et al.* The progress of gut microbiome research related to brain disorders. *J. Neuroinflamm.* **17**, 25 (2020).
56. Fang, X. Potential role of gut microbiota and tissue barriers in Parkinson's disease and amyotrophic lateral sclerosis. *Int. J. Neurosci.* **126**, 771–776 (2016).
57. Boddy, S. L. *et al.* The gut microbiome: a key player in the complexity of amyotrophic lateral sclerosis (ALS). *BMC Med.* **19**, 13 (2021).
58. Kincaid, H. J., Nagpal, R. & Yadav, H. Diet-microbiota-brain axis in Alzheimer's disease. *Ann. Nutr. Metab.* **77**(Suppl 2), 21–27 (2021).
59. Blacher, E., Levy, M., Tatirovsky, E. & Elinav, E. Microbiome-modulated metabolites at the interface of host immunity. *J. Immunol.* **198**, 572–580 (2017).
60. Chang, C., Lin, C. & Lane, H. d-glutamate and gut microbiota in Alzheimer's disease. *Int. J. Mol. Sci.* **21**, 2676 (2020).
61. Mazzini, L. *et al.* Potential role of gut microbiota in ALS pathogenesis and possible novel therapeutic strategies. *J. Clin. Gastroenterol.* **52**, S68–S70 (2018).
62. Han, N. *et al.* Rapid turnover and short-term blooms of *Escherichia coli* in the human gut. *J. Bacteriol.* **206**, e0023923-23 (2024).
63. Qi, Y., Yu, L., Tian, F., Zhao, J. & Zhai, Q. In vitro models to study human gut-microbiota interactions: Applications, advances, and limitations. *Microbiol. Res.* **270**, 127336 (2023).
64. Wenzel, T. J. & Chisholm, C. D. Using NMR spectroscopic methods to determine enantiomeric purity and assign absolute stereochemistry. *Prog. Nucl. Magn. Reson. Spectrosc.* **59**, 1–63 (2011).
65. Farjon, J. & Giraud, N. 1H NMR analyses of enantiomeric mixtures using chiral liquid crystals. *Curr. Opin. Colloid Interface Sci.* **33**, 1–8 (2018).
66. Xing, Y., Li, X., Guo, X. & Cui, Y. Simultaneous determination of 18 d-amino acids in rat plasma by an ultrahigh-performance liquid chromatography-tandem mass spectrometry method: Application to explore the potential relationship between Alzheimer's disease and d-amino acid level alterations. *Anal. Bioanal. Chem.* **408**, 141–150 (2016).
67. Danielsen, M., Nebel, C. & Dalsgaard, T. K. Simultaneous determination of L- and D-amino acids in proteins: A sensitive method using hydrolysis in deuterated acid and liquid chromatography-tandem mass spectrometry analysis. *Foods* **9**, 309 (2020).
68. Aizawa, S., Kidani, T., Takada, S. & Ofusa, Y. Simple resolution of enantiomeric NMR signals of α-amino acids by using samarium(III) nitrate with L-tartarate. *Chirality* **27**, 353–357 (2015).
69. Erickson, D. W. *et al.* A global resource allocation strategy governs growth transition kinetics of *Escherichia coli*. *Nature* **551**, 119–123 (2017).
70. Zhu, M. & Dai, X. Stringent response ensures the timely adaptation of bacterial growth to nutrient downshift. *Nat. Commun.* **14**, 467 (2023).
71. McLaggan, D., Naprstek, J., Buurman, E. T. & Epstein, W. Interdependence of K+ and glutamate accumulation during osmotic adaptation of *Escherichia coli*. *J. Biol. Chem.* **269**, 1911–1917 (1994).
72. Sanz-Jiménez, A. *et al.* High-throughput determination of dry mass of single bacterial cells by ultrathin membrane resonators. *Commun. Biol.* **5**, 1227 (2022).
73. Burkovski, A., Weil, B. & Krämer, R. Glutamate excretion in *Escherichia coli*: Dependency on thereIA andspoT genotype. *Arch. Microbiol.* **164**, 24–28 (1995).
74. Paczia, N. *et al.* Extensive exometabolome analysis reveals extended overflow metabolism in various microorganisms. *Microbial. Cell Factor.* **11**, 122 (2012).
75. Palla, G., Marchelli, R., Dossena, A. & Casnati, G. Occurrence of D-amino acids in food: Detection by capillary gas chromatography and by reversed-phase high-performance liquid chromatography with L-phenylalaninamides as chiral selectors. *J. Chromatogr. A* **475**, 45–53 (1989).
76. Jin, D., Miyahara, T., Oe, T. & Toyo'oka, T. Determination ofd-amino acids labeled with fluorescent chiral reagents, R (−)- and S(+)-4-(3-isothiocyanatopyrrolidin-1-yl)-7- (N, N-dime thylaminosulfonyl)-2,1,3-benzoxadiazoles, in biological and food samples by liquid chromatography. *Anal. Biochem.* **269**, 124–132 (1999).
77. Brückner, H. & Hausch, M. Gas chromatographic detection of D-amino acids as common constituents of fermented foods. *Chromatographia* **28**, 487–492 (1989).
78. Marcone, G. L., Rosini, E., Crespi, E. & Pollegioni, L. D-amino acids in foods. *Appl. Microbiol. Biotechnol.* **104**, 555–574 (2020).
79. Lim, D. *et al.* Calcium homeostasis and mitochondrial dysfunction in striatal neurons of Huntington disease. *J. Biol. Chem.* **283**, 5780–5789 (2008).
80. Smith, E. F., Shaw, P. J. & De Vos, K. J. The role of mitochondria in amyotrophic lateral sclerosis. *Neurosci. Lett.* **710**, 132933 (2019).
81. Siemers, K. M., Klein, A. K. & Baack, M. L. Mitochondrial dysfunction in PCOS: Insights into reproductive organ pathophysiology. *Int. J. Mol. Sci.* **24** (2023).
82. Guo, C., Sun, L., Chen, X. & Zhang, D. Oxidative stress, mitochondrial damage and neurodegenerative diseases. *Neural Regen. Res.* **8**, 2003–2014 (2013).
83. Sasaki, S. & Iwata, M. Mitochondrial alterations in the spinal cord of patients with sporadic amyotrophic lateral sclerosis. *J. Neuropathol. Exp. Neurol.* **66**, 10–16 (2007).
84. Atsumi, T. The ultrastructure of intramuscular nerves in amyotrophic lateral sclerosis. *Acta Neuropathol.* **55**, 193–198 (1981).
85. Zhang, W., Chen, Y. & Pei, H. C1q and central nervous system disorders. *Front. Immunol.* **14**, 1145649 (2023).
86. Gomez-Arboledas, A., Acharya, M. M. & Tenner, A. J. The role of complement in synaptic pruning and neurodegeneration. *Immunotargets Ther.* **10**, 373–386 (2021).
87. Kouser, L. *et al.* Emerging and novel functions of complement protein C1q. *Front. Immunol.* **6**, 317 (2015).
88. van de Bovenkamp, F. S., Dijkstra, D. J., van Kooten, C., Gelderman, K. A. & Trouw, L. A. Circulating C1q levels in health and disease, more than just a biomarker. *Mol. Immunol.* **140**, 206–216 (2021).
89. Eggleton, P., Reid, K. B. & Tenner, A. J. C1q-how many functions? How many receptors?. *Trends Cell Biol.* **8**, 428–431 (1998).
90. Eggleton, P., Tenner, A. J. & Reid, K. B. C1q receptors. *Clin. Exp. Immunol.* **120**, 406–412 (2000).

91. Datta, D. *et al.* Classical complement cascade initiating C1q protein within neurons in the aged rhesus macaque dorsolateral prefrontal cortex. *J. Neuroinflamm.* **17**, 8 (2020).
92. Bie, B., Wu, J., Foss, J. F. & Naguib, M. Activation of mGluR1 mediates C1q-dependent microglial phagocytosis of glutamatergic synapses in Alzheimer's rodent models. *Mol. Neurobiol.* **56**, 5568–5585 (2019).
93. Thielens, N. M., Tedesco, F., Bohlson, S. S., Gaboriaud, C. & Tenner, A. J. C1q: A fresh look upon an old molecule. *Mol. Immunol.* **89**, 73–83 (2017).
94. Lansita, J. A. *et al.* Nonclinical development of ANX005: A humanized anti-C1q antibody for treatment of autoimmune and neurodegenerative diseases. *Int. J. Toxicol.* **36**, 449–462 (2017).
95. Chung, H. *et al.* Microglia mediate neurocognitive deficits by eliminating C1q-tagged synapses in sepsis-associated encephalopathy. *Sci. Adv.* **9**, 7806 (2023).
96. Dejanovic, B. *et al.* Complement C1q-dependent excitatory and inhibitory synapse elimination by astrocytes and microglia in Alzheimer's disease mouse models. *Nat. Aging* **2**, 837–850 (2022).
97. Chiò, A. *et al.* Global epidemiology of amyotrophic lateral sclerosis: A systematic review of the published literature. *Neuroepidemiology* **41**, 118–130 (2013).
98. Mehta, P. *et al.* Prevalence of amyotrophic lateral sclerosis—United States, 2012–2013. *MMWR Surveill. Summ.* **65**, 1–12 (2016).
99. Mehta, P. *et al.* Prevalence of amyotrophic lateral sclerosis in the United States using established and novel methodologies, 2017. *Amyotroph. Lateral Scler. Frontotemp. Degener.* **24**, 108–116 (2023).
100. Payne, B. A. I. & Chinnery, P. F. Mitochondrial dysfunction in aging: Much progress but many unresolved questions. *Biochim. Biophys. Acta* **1847**, 1347–1353 (2015).
101. Mead, R. J., Shan, N., Reiser, H. J., Marshall, F. & Shaw, P. J. Amyotrophic lateral sclerosis: A neurodegenerative disorder poised for successful therapeutic translation. *Nat. Rev. Drug Discov.* **22**, 185–212 (2023).
102. Lamanauskas, N. & Nistri, A. Riluzole blocks persistent Na+ and Ca2+ currents and modulates release of glutamate via presynaptic NMDA receptors on neonatal rat hypoglossal motoneurons in vitro. *Eur. J. Neurosci.* **27**, 2501–2514 (2008).
103. Monselise, E. B. I. D-aminio acids are signeling agents under stress, that broadly impact preventive medicine. *Preprints*. 2019090334 (2019).
104. Binenbaum, Z., Klyman, E. & Fishov, I. Division-associated changes in membrane viscosity of *Escherichia coli*. *Biochimie* **81**, 921–929 (1999).
105. Teixeira, J., Tiritan, M. E., Pinto, M. M. M. & Fernandes, C. Chiral stationary phases for liquid chromatography: Recent developments. *Molecules* **24**, 865 (2019).
106. Batushansky, A., Lopes, E. B. P., Zhu, S., Humphries, K. M. & Griffin, T. M. GC-MS method for metabolic profiling of mouse femoral head articular cartilage reveals distinct effects of tissue culture and development. *Osteoarthr. Cartil.* **27**, 1361–1371 (2019).

Acknowledgements

We want to thank the late Prof. Daniel Kost and Aliza Levkovitz, for the ^{15}N-NMR spectrometric research work done together for over 30 years. It was the basis that led to the present research work. We wish to thank Prof. Dudy Bar-Zvi, Dr. Amira Rudi, Engineer Itsik Cohen (Bruker Israel), Prof. Adrian Israelson, Prof. Sen-Ichi Aizawa, Prof. David Avnir, Prof. Yossi Paltiel, Prof Itzhak Mizrahi and, Dr. Galit Yehezkel for their helpful comments. We wish to thank for helpful assistance: Dorit van-Moppes, Eyal Ben-Yehuda and Alina Katz, Library Information Specialists and Oded Shaul Ben-Izhak for Graphic editing.
This article is dedicated to my dear husband and best friend, the late Moshe Melech Ben-Izhak who courageously withstood ALS disease from March18th 2018 till January19th 2021 and inspired everyone around him. May you rest in peace as I am keeping my promise to you.

Author contributions

E.B.I.M.—developed the concept and the working hypothesis, designed and performed the research, and drew the explanatory scheme; M.V. and I.F.—assisted and advised in planning microbiology experiments; T.S.—performed and analyzed the NMR experiments, including graphical presentation; A.B.—developed and performed sample preparation for LC–MS, conducted and analyzed LC–MS measurements and prepared figures. All authors listed have made a substantial, direct, and intellectual contribution to the writing of the manuscript, and approved it for publication.

Competing interests

The authors declare no competing interests.

Additional information

Supplementary Information The online version contains supplementary material available at https://doi.org/10.1038/s41598-024-68645-8.

Correspondence and requests for materials should be addressed to E.B.-I.M. or I.F.